

STOCHASTIC MODELING OF FATIGUE CRACK PROPAGATION IN CONCRETE BEAMS USING MARKOV CHAIN SIMULATION

SUMIT SINGH THAKUR*, PERVAIZ FATHIMA K.M.†

*Indian Institute of Technology Jammu
Jammu and Kashmir, India
e-mail: sumit.thakur@iitjammu.ac.in

†Indian Institute of Technology Jammu
Jammu and Kashmir, India
e-mail: pervaiz.khattoon@iitjammu.ac.in

Key words: Stochastic Modelling, Markov Chain, Concrete, Fatigue crack propagation

Abstract. Fatigue crack growth is a critical issue in the field of structural engineering, including concrete structures. Concrete is a heterogeneous quasi-brittle material and its behaviour is affected by various factors such as loading conditions, material properties, and environmental factors. Fatigue crack propagation in concrete is regarded as a random phenomenon because it depends on various factors that behave in a variable or unpredictable manner. These factors include the characteristics of the concrete, such as its stiffness and strength, dimensions, morphology, crack path, and loading conditions. It is essential to accurately model and predict the uncertain process of fatigue crack growth for designing and maintaining structures such as bridges, nuclear power plants, and offshore structures. In order to address this issue, the fatigue crack growth in concrete is modeled using Markov Chain simulation. The transition number of cycles from stable to unstable crack growth region is estimated by optimizing parameters of Paris' and Forman's laws. Also, the crack length prediction model is developed based on the principle of Markov chains.

1 INTRODUCTION

The fatigue crack propagation typically is represented as the rate of crack growth with the number of cycles versus the stress intensity factor range in which three different stages are demarcated as shown in Fig. 1. The first stage (regime A) is the short crack growth regime where the crack growth rate is dependent on the material microstructure. The second stage (regime B) is the stable crack growth regime where the Paris' law is applicable. The third and final stage (regime C) is characterised by a rapid increase in crack growth rate leading to fracture.

A Markov chain or Markov process is a

probabilistic framework that characterizes a series of potential occurrences. In this framework, the likelihood of each event occurring is influenced solely by the state reached in the preceding event. In simpler terms, one can conceive of it as "The forthcoming outcome is solely determined by the present circumstances." [1].

Markov processes are often employed to analyze fatigue crack propagation in metals [2–4]. The study of fatigue crack growth in concrete using Markov processes has been relatively limited, despite the significant similarity between fatigue crack growth and Markov's chain. Concrete exhibits a more random cracking pattern compared to metals due to its heterogeneous microstructure. The presence of aggre-

gate boundaries in concrete leads to the coalescence of initial cracks. Additionally, the fracture process zone ahead of the crack tip in concrete is not fully understood, unlike the plastic zone in metals [5]. Paris' and Forman's laws, commonly used for fatigue crack growth in metals, do not accurately apply to concrete. Therefore, size-adjusted versions of these laws are typically used for concrete [7].

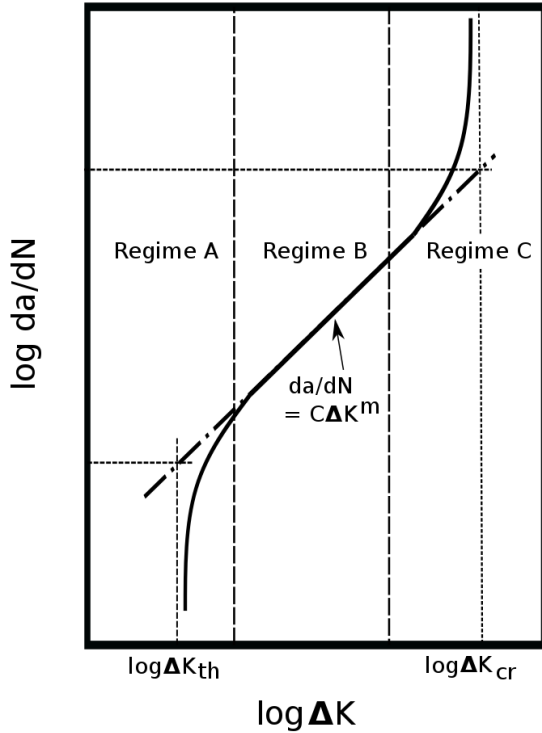


Figure 1: Typical plot of crack growth rate with respect to the stress intensity range where the Paris–Erdogan equation fits the central, linear region of Regime B.

This work aims to stochastically assess the transition time, which represents the shift from stable to unstable crack growth, and predict the fatigue crack length in concrete based on the number of cycles using the Markov chain simulation. The proposed model takes into account crack growth regimes B and C and their transition allowing for a more accurate representation of the complex nature of the fatigue crack growth process. A regime-switching model is used to express the transition number of cycles between regions B and C. Also, the fatigue crack path is predicted using Paris' law. The

proposed model is demonstrated using experimental data from available literature on crack growth rate with stress intensity factor range for three-point bend experimental tests of plain concrete beams to develop a prior distribution of the crack growth parameters. The proposed model has several advantages over traditional deterministic models for fatigue crack growth in concrete as it is based on a rigorous mathematical framework that can accurately represent the stochastic nature of the fatigue crack growth process and it accounts for different crack growth regimes and their transitions, which allows for a more accurate representation of the complex nature of the fatigue crack growth process. The model can also aid in developing more robust models for concrete fatigue analysis.

2 METHODOLOGY

2.1 Mathematical framework

Paris' law [6] and Forman's law [8] are both mathematical equations related to material fatigue and the behavior of materials under cyclic loading, but they focus on different aspects and have distinct applications.

Paris' law, also known as the Paris-Erdogan equation is a mathematical relationship that describes the growth rate of fatigue cracks in materials. It specifically focuses on the propagation of small cracks within a material subjected to cyclic loading. The law provides a way to predict how fast a crack will grow in a material over time, considering factors like stress intensity, crack size, and the material's properties [9]. The Paris' law is given by:

$$\frac{da}{dN} = C_1(\Delta K)^{m_1} \quad (1)$$

$$\text{where, } \Delta K = (\Delta\sigma) \cdot Y\left(\frac{a}{D}\right) \cdot \sqrt{\pi a}$$

$\Delta\sigma$ is the applied stress range in the fatigue tests, $Y(a/D)$ is the geometric factor which depends on the ratio $\frac{a}{D}$, where a is the crack length and D is the depth of the specimen. C_1 and m_1 are the Paris' law parameters. N is the number of cycles of fatigue loading.

In essence, Paris' law is used to estimate the rate at which a fatigue crack will advance in a material, which is essential for assessing the remaining useful life of structures and components subjected to cyclic loading, such as aircraft wings, pressure vessels, and pipelines [10].

Forman's law emphasizes the concept that the strength or resistance of a material decreases as it experiences a higher number of stress cycles. It focuses on the overall degradation of material properties due to repeated loading and unloading. Forman's law is particularly relevant when dealing with materials subjected to low-cycle fatigue, where the stress levels are relatively high [11, 12]. Forman's law is given by:

$$\frac{da}{dN} = \frac{C_2(\Delta K)^{m_2}}{(1-R)K_c - \Delta K} \quad (2)$$

where R is the ratio of the minimum to maximum stress during fatigue loading. C_2 and m_2 are the Forman's law parameters. K_C is the size-dependent equivalent fracture toughness.

Paris' law is concerned with the growth rate of fatigue cracks in materials, while Forman law deals with the reduction in material strength due to repeated loading cycles. Both laws provide valuable insights into the behavior of materials under cyclic loading conditions, but they address different aspects of material fatigue and have distinct applications in engineering and materials science. Paris' law corresponds to the stable crack growth region, and Forman's law corresponds to the region of unstable rapid crack growth [13].

The Paris' and Forman's laws are not directly applicable to concrete [7]. Rather, their size adjusted versions are relatively better applicable as in Eq. 3 and Eq. 4, respectively.

$$\frac{da}{dN} = C_1 \left(\frac{\Delta K}{K_c} \right)^{m_1} \quad (3)$$

$$\frac{da}{dN} = \frac{C_2 \left(\frac{\Delta K}{K_c} \right)^{m_2}}{(1-R)K_c - \frac{\Delta K}{K_c}} \quad (4)$$

where K_C is the size-dependent equivalent fracture toughness which is related to the constant

fracture toughness, K_f , by [7].

$$K_c = K_f \left(\frac{\beta}{1+\beta} \right)^{\frac{1}{2}}$$

where β is the brittleness number defined as $\frac{d}{d_0}$, where d is the structural size and d_0 is the transitional size.

To determine the number of cycles corresponding to the transition from regime B to C, a hypothesis is considered: The relationship between the logarithm of crack growth rate $\log(\frac{da}{dN})$ and the logarithm of the stress intensity factor range $\log(\frac{\Delta K}{K_c})$ shows a linear pattern during stable crack growth. However, in the unstable crack growth region, this relationship transforms into a shape resembling an exponential curve. This hypothesis is shown as transition theory in Fig 2. The crack growth rate curve is a combination of the size-adjusted Paris region, which follows a linear pattern, and the size-adjusted Forman region, which exhibits a non-linear behavior. The point where these two regions intersect corresponds to the cycle count at which the crack propagation shifts from a stable regime to an unstable one.

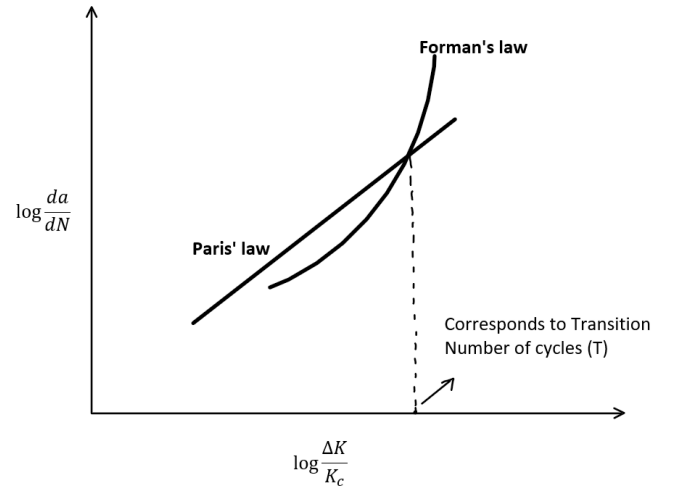


Figure 2: Proposed transition theory which is a combination of size-adjusted Paris region (Linear) and size-adjusted Forman region (Non-Linear). Their intersection corresponds to the transition number of cycles (T), i.e., the number of cycles at which the crack propagation goes from stable to unstable region

Based on this transition theory, it is suggested that the point where the curve transitions

from the linear pattern of Paris' law (representing stable growth) to the exponential pattern of Forman's law (representing unstable growth) indicates the shift from stable to unstable crack growth. The parameters of the Paris' law (m_1, C_1) and Forman's law (m_2, C_2) influence the gradients and intercepts of these equations, respectively.

In the second part of this work, an algorithm is developed to predict the path of crack propagation based on Markov's process, utilizing these optimized parameters. This algorithm aims to predict the path of crack propagation. For the sake of simplicity, the mathematical modeling of the second part is restricted to the use of Paris' law only.

The specific details of both algorithms are explained in the following subsections. These algorithms aim to fine-tune the Paris' and Forman's laws parameters for accurate predictions and then use Paris's law parameters to simulate the crack with number of cycles of loading.

2.2 Algorithms

Algorithm 1: Estimating number of cycles at transition by optimising Paris' and Forman's parameters

- Get the the experimental value of crack length a_{exp}^N vs number of cycles N .
- Define an objective function f given below in Eq. 5 that calculates the sum of square of differences between the predicted crack length using Paris' and Forman's equations (with parameters m_1, C_1, T, m_2, C_2) and the actual experimental crack length a_{exp}^N .

$$f = f_1 + f_2 \quad (5)$$

$$\text{where, } f_1 = \sum_{N=0}^T (a^N(m_1, C_1, N) - a_{\text{exp}}^N)^2$$

$$\text{and, } f_2 = \sum_{i=T}^{N_f} (a^N(m_2, C_2, N) - a_{\text{exp}}^N)^2$$

where, $a^N(m_1, C_1, N)$ corresponds to theoretical crack length calculated as per size adjusted Paris' law at N number of cycles. Similarly, $a^N(m_2, C_2, N)$ corresponds to the theoretical crack length as per size adjusted Forman's law. N_f denotes the number of cycles at which the specimen fails

- Minimize the objective function f to find the best-fit values for the parameters m_1^* , C_1^* , T^* , m_2^* , and C_2^* , which optimize the agreement between predicted and actual crack growth rates.

Algorithm 2: Predicting Crack Length Using Optimized Parameters

- Get 'n' experimental points for crack length a versus the number of cycles N . 'n' depends on number of experimental data points available for a particular specimen.
- Use the optimized values of m_1 and C_1 to generate 10 sets of random parameters (m_1, C_1) using the mean and standard deviation through Monte Carlo simulation.
- Starting from the first experimental point, generate 10 crack length versus cycles curves using the Paris' law and the parameter sets generated in the above step.
- Calculate a distance optimization function (f_d)

$$f_d = \sum_{N=0}^{N_f} \sum_{i=1}^{10} ((a_i(m_i, C_i, N) - a_{i,\text{exp}}(N))^2) \quad (6)$$

for each of the 10 curves compared to the experimental curve, and select the four curves that are closest.

- Randomly pick one of the four nearest curves and move to the next experimental point (N_2).
- Repeat the above step by generating 10 curves for each point, selecting the one with the least distance, and moving to the subsequent experimental points (N_3, N_4 , and so on). Each

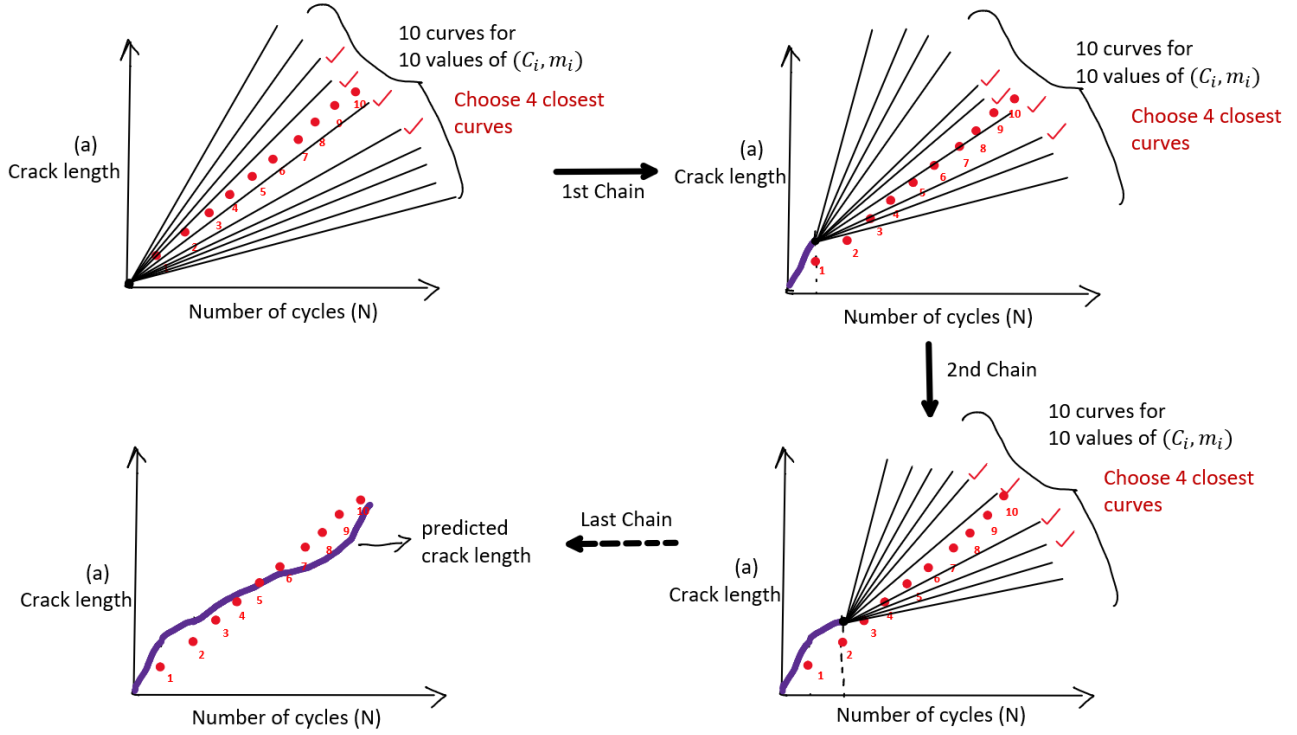


Figure 3: Schematic illustration of steps involved in Algorithm-2. Each step serves as Markov's chain

Table 1: Details of the beam specimens considered for the study (all lengths are in mm and all load are in kN)

| Specimen | Thickness | Depth | Length | span | Initial Notch | Peak Load | N_f |
|-------------------------------|-----------|-------|--------|-------|---------------|-----------|-------|
| Shah and Kishen [14] (Small) | 50 | 76 | 241 | 190 | 15.2 | 4.46 | 11642 |
| Shah and Kishen [14] (Medium) | 50 | 152 | 431 | 380 | 30.4 | 6.78 | 11128 |
| Shah and Kishen [14] (Large) | 50 | 306 | 810 | 760 | 60.8 | 11.70 | 12530 |
| Bazant and Xu [7] (Small) | 38.1 | 38.1 | 101.6 | 95.25 | 6.35 | 4.08 | 939 |
| Bazant and Xu [7] (Medium) | 38.1 | 76.2 | 203.2 | 190.5 | 12.7 | 6.71 | 1286 |
| Bazant and Xu [7] (Large) | 38.1 | 152.4 | 406.4 | 381 | 25.4 | 11.65 | 1083 |

step serves as Markov's chain. These steps are shown schematically in Fig. 3.

- Repeat this process for all experimental points, generating a series of curves that predict the crack growth path based on the optimized parameters.

The theoretical N value as a function of crack length a is obtained by numerical integration as given in Eq. 7 using the limit of sum method.

$$N(a) = (a - a_0) \lim_{n \rightarrow \infty} \frac{1}{n} \sum_{a=a_0}^{a_0+(i-1)h} f(a) \quad (7)$$

$$\text{where, } f(a) = \frac{1}{C_1 \cdot \left(\frac{\Delta\sigma}{K_c} \cdot Y \left(\frac{a}{D} \right) \cdot \sqrt{\pi a} \right)^{m_1}}$$

Then, the inverse function of N , denoted as $g^{-1}(N)$, is generated to obtain the predicted crack length a as a function of N , i.e. $a(N) = g^{-1}(N)$.

This mathematical operation is performed using MATLAB R2022b.

Table 2: Optimised Paris' and Forman's law parameters with transition number of cycles

| Specimen | m_{1exp} | $\log C_{1exp}$ | m_1^* | $\log C_1^*$ | m_2^* | $\log C_2^*$ | T^* | m_1 error |
|-------------------------------|------------|-----------------|---------|--------------|---------|--------------|-------|-------------|
| Shah and Kishen [14] (Small) | 6 | -9.7 | 5.73 | -7.25 | 6.14 | -8.46 | 8353 | 4.50% |
| Shah and Kishen [14] (Medium) | 4.5 | -8.3 | 4.91 | -6.07 | 4.21 | -7.58 | 8376 | 9.11% |
| Shah and Kishen [14] (Large) | 4.8 | -9.0 | 4.16 | -6.27 | 4.69 | -7.98 | 9464 | 13.35% |
| Bazant and Xu [7] (Small) | 10.6 | -18.3 | 10.32 | -18.94 | 11.26 | -20.36 | 689 | 2.64% |
| Bazant and Xu [7] (Medium) | 10.6 | -18.4 | 9.80 | -19.56 | 10.75 | -20.78 | 921 | 7.54% |
| Bazant and Xu [7] (Large) | 10.6 | -18.4 | 12.51 | -23.40 | 13.24 | -24.22 | 845 | 11.13% |

3 APPLICATION OF THE PROPOSED METHODOLOGY

The two algorithms described in Section 2.2 needed to be executed by crack growth data. For this, data of the 3-point bend test is taken from two sources, Shah and Kishen [14]; and Bazant and Xu [7]. The experimental data was available for three sizes of beam specimens from both the sources, viz. small, medium, and large. The sizes of specimens and the loading conditions of fatigue tests are presented in Table 1. The geometric shape function for the given 3-point beams with span to depth ratio 2.5 is given by:

$$Y\left(\frac{a}{D}\right) = \left(1 - \frac{a}{D}\right)^{-\frac{3}{2}} \cdot \left(1 - 2.5 \cdot \frac{a}{D} + 4.49 \cdot \left(\frac{a}{D}\right)^2 - 3.98 \cdot \left(\frac{a}{D}\right)^3 + 1.33 \cdot \left(\frac{a}{D}\right)^4\right)$$

The data from both sources was incorporated into the algorithm to optimize the values of the Paris and Forman's law parameters, thus generating the transition number of cycles.

For Algorithm-1, the input parameters included the dimensions of the beam, initial notch length, loading parameters, geometric factor, and the brittleness number β . The values of β were considered as 0.052, 0.104, and 0.209 for small, medium, and large specimens in the respective order [7]. The input parameters for each specimen were taken from Table 1.

Algorithm-1, aimed at determining the transition number of cycles, was executed using a non linear least-squares solver (lsqnonlin) from the R2022b version of MATLAB software.

After finding the optimized values of the parameters by executing Algorithm-1, optimized Paris' law parameters were incorporated to exe-

cute Algorithm-2 and predict the crack length against the experimental crack length for the respective specimens of the study. The input parameters for crack length prediction included the optimized parameters of Paris' law and the geometric factor. Ten sets of values for m_1 and C_1 were generated using Monte Carlo simulation, with the optimized values as the mean and a 10% standard deviation following a normal distribution. This randomization was performed to align with the problem-solving heuristic of following a greedy algorithm, which entails making locally optimal choices at each stage of the Markov chain [15].

4 RESULTS AND DISCUSSIONS

The proposed methodology was implemented as described in Section 3. For the first part of the work, the optimized parameters m_1^* , $\log C_1^*$, m_2^* , and $\log C_2^*$, along with the transition number of cycles (T^*), are reported in Table 2 along with the experimental values of m_{1exp} and $\log C_{1exp}$ for all the specimens under consideration. The errors in the m_1 values are found to be 4.50%, 9.11%, and 13.35% for data from Shah and Kishen [14] for small, medium, and large-sized specimens, respectively. The corresponding errors for data from Bazant and Xu [7] were found to be 2.64%, 7.54%, and 11.13%. It is important to note that the parameters of Forman's law were not reported in either of the experimental studies. It is observed that the transition model predicts well for small-sized specimens compared to large-sized specimens.

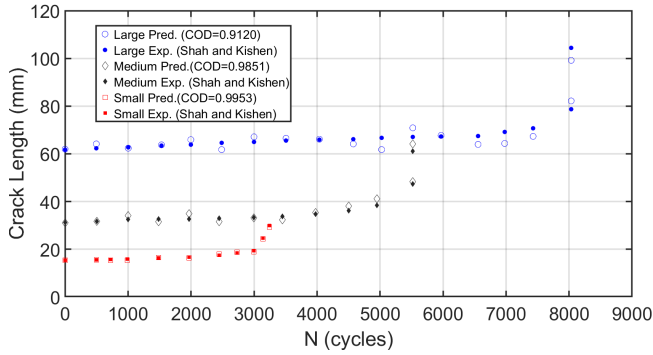


Figure 4: Predicted crack length against experimental data set for three sets of specimens conducted by Shah and Kishen [14].

For the second part of the work, the predicted crack lengths for all respective experimental data sets are depicted in Fig. 4 (for Shah and Kishen [14]) and Fig.5 (for Bazant and Xu [7]). Fig. 4 includes 11, 13, and 18 data points for small, medium, and large-sized specimens, respectively. In contrast, Fig. 5 involved 13, 13, and 12 data points for small, medium, and large-sized specimens, respectively.

In the case of Shah and Kishen [14], the coefficient of determination (COD) for predicted crack length was noted as 0.9956, 0.9851, and 0.9120 for small, medium, and large-sized specimens, respectively. Likewise, for Bazant and Xu [7], the coefficient of determination for predicted crack length was 0.9970, 0.9812, and 0.9721 for small, medium, and large-sized specimens, respectively.

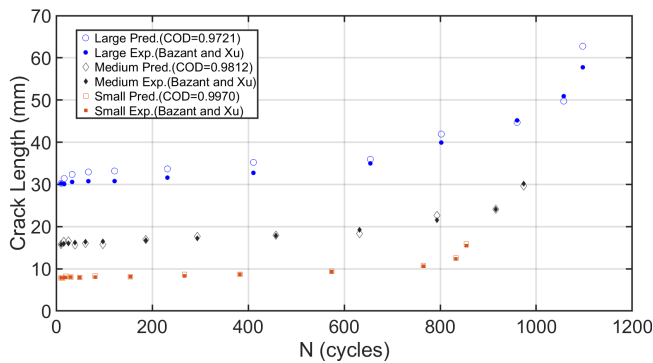


Figure 5: Predicted crack length against experimental data set for three sets of specimens conducted by Bazant and Xu [7] [7].

It is evident that the proposed model demonstrates better accuracy in predicting crack paths for smaller-sized specimens compared to larger-sized ones. Additionally, the model's accuracy is more pronounced at lower cycle numbers, whereas its predictive capability diminishes at higher cycle numbers. This discrepancy might have arisen from the omission of Forman's law in the crack prediction model, which is more relevant for higher cycle numbers.

5 CONCLUSIONS

In the first part of this work, the number of cycles corresponding to the shift from the stable crack growth region to the unstable crack growth region (transition number of cycles) is evaluated using the proposed transition theory, which involves size-adjusted Paris' and Forman's laws for concrete. The experimental data was obtained from two separate sources in the literature, and it demonstrates good agreement with the optimized parameters.

Predicting crack length for fatigue in concrete using Markov chain simulation holds several significant advantages and benefits in the field of concrete. The significance of predicting crack length for fatigue in concrete using Markov chain simulation lies in its ability to provide accurate, probabilistic, and long-term predictions that enable better decision-making for the design, maintenance, and safety of concrete structures. In the second part of the work, crack length is predicted for the same two experimental data sets using the principle of Markov chain simulation. The respective predicted crack lengths were obtained and plotted against the experimental values with good coefficients of determination. The findings indicate that the predictions are more accurate for smaller-sized specimens when compared to larger ones. Additionally, the accuracy of predictions was higher for a lower number of fatigue cycles compared to a higher number of fatigue cycles.

REFERENCES

- [1] Gagniuc and Paul A. (2017). *Markov Chains: From Theory to Implementation and Experimentation.*, USA, NJ: John Wiley Sons. pp. 1–235. ISBN 978-1-119-38755-8.
- [2] Hashmi, M. H. (2023). *Fractal and probabilistic analysis on fatigue crack growth rate of metallic materials*, (Doctoral dissertation, Universiti Teknologi Malaysia).
- [3] Li, Y. Z., Zhu, S. P., Liao, D., and Niu, X. P. (2020). Probabilistic modeling of fatigue crack growth and experimental verification. *Engineering Failure Analysis*, 118, 104862.
- [4] Ben Abdesslem, A., Azaïs, R., Touzet-Cortina, M., Gégout-Petit, A., and Puigali, M. (2016). Stochastic modelling and prediction of fatigue crack propagation using piecewise-deterministic Markov processes. *Proceedings of the Institution of Mechanical Engineers, Part O: Journal of Risk and Reliability*, 230(4), 405-416.
- [5] Rongxin Zhou, Yong Lu, Li-Ge Wang, Han-Mei Chen, (2021). Mesoscale modelling of size effect on the evolution of fracture process zone in concrete. *Engineering Fracture Mechanics*, Volume 245, 2021, 107559, ISSN 0013-7944.
- [6] Paris, P., and Erdogan, F. (December 1, 1963). A Critical Analysis of Crack Propagation Laws. *ASME. J. Basic Eng.* 1963; 85(4): 528–533.
- [7] Bažant, Z.P., and Xu, K. 1991. Size effect in fatigue fracture of concrete. *ACI Materials Journal*, 88(4), 390-399.
- [8] Forman, R. G., Kearney, V. E., and Engle, R. M. (1967). Numerical Analysis of Crack Propagation in Cyclic-Loaded Structures. *ASME. J. Basic Eng.* 1967; 89(3): 459–463.
- [9] Allegri, G. (2020). A unified formulation for fatigue crack onset and growth via cohesive zone modelling. *Journal of the Mechanics and Physics of Solids*, 138, 103900.
- [10] Venugopal, A., Mohammad, R., Koslan, M. F. S., Shafie, A., Ali, A. B., and Eugene, O. (2021). Crack Growth Prediction on Critical Component for Structure Life Extension of Royal Malaysian Air Force (RMAF) Sukhoi Su-30MKM. *Metals*, 11(9), 1453.
- [11] Tavares, S. M., and De Castro, P. M. (2019). *Damage tolerance of metallic aircraft structures: materials and numerical modelling.*, Berlin/Heidelberg, Germany: Springer (2019).
- [12] Schreiber, C., Müller, R., and Kuhn, C. (2021). Phase field simulation of fatigue crack propagation under complex load situations. *Archive of Applied Mechanics*, 91, 563-577.
- [13] Pugno, N., Ciavarella, M., Cornetti, P., and Carpinteri, A. (2006). A generalized Paris' law for fatigue crack growth. *Journal of the Mechanics and Physics of Solids*, 54(7), 1333-1349.
- [14] Santosh G. Shah, and J.M. Chandra Kishen, 2012. Use of acoustic emissions in flexural fatigue crack growth studies on concrete. *Engineering Fracture Mechanics*, Volume 87, 2012, Pages 36-47.
- [15] Mousavi, S., Bhambar, S., and England, M. (2023). An iterated greedy algorithm with variable reconstruction size for the obnoxious p-median problem. *International Transactions in Operational Research* (2023).